© 2010 Chinese Ocean Engineering Society, ISSN 0890-5487

Probability of Sediment Incipient Motion Under Complex Flows*

LIU Chun-rong (刘春嵘)[a,1], DENG Li-ying (邓丽颖)[a] and HUHE Aode (呼和敖德)[b]

[a] *College of Mechanics and Aerospace, Hunan University, Changsha 410082, China*

[b] *Institute of Mechanics, Chinese Academy of Sciences, Beijing 100080, China*

(Received 19 January 2009; received revised form 1 July 2009; accepted 5 November 2009)

ABSTRACT

Presented in this paper is a mathematical model to calculate the probability of the sediment incipient motion, in which the effects of the fluctuating pressure and the seepage are considered. The instantaneous bed shear velocity and the pressure gradient on the bed downstream of the backward-facing step flow are obtained according to the PIV measurements. It is found that the instantaneous pressure gradient on the bed obeys normal distribution. The probability of the sediment incipient motion on the bed downstream of the backward-facing step flow is given by the mathematical model. The predicted results agree well with the experiment in the region downstream of the reattachment point while a large discrepancy between the theory and experiment is seen in the region near the reattachment point. The possible reasons for this discrepancy are discussed.

Key words: *probability; sediment incipience; backward-facing step flow; seepage; pressure*

1. Introduction

The critical condition of sediment incipient motion is important for the study of sediment transport and local scouring process and it has been concerned by numerous researchers. Most work about sediment transport connected the sediment incipience with bed shear stress. The critical incipient shear stress can be well defined for the unidirectional turbulent stream flows. Up to now, there are a large number of empirical formulae developed (van Rijn, 1984; Dou, 2000; Cheng, 2004; Cao *et al.*, 2006) to evaluate the critical incipient shear stress of sediment with different properties (cohesive or cohesionless). It is noted that these empirical formulae are derived based on the experiments under unidirectional stream flows.

The critical incipient condition under complex flows, which have both flow separation and reattachment associated with large scale vortices, has attracted many investigators' attention. At present, most researches on the local scouring under complex flows or waves still adopt traditional formula obtained under unidirectional flow to describe the critical condition of sediment incipience (Zhou *et al.*, 2001; Zhao and Teng, 2001; Chen *et al.*, 2004; Liang *et al.*, 2005). However, Lyn (1995) and Liu and Huhe (2003) studied sediment incipience under turbulence generated by oscillating grid and reported that sediment grains could be picked up under the condition of zero mean bed shear stress. These studies imply that the sediment incipience can not be only attributed to bed shear stress under complex flows.

* This work was financially supported by the National Natural Science Foundation of China (Grant No. 10602017)

1 Corresponding author. E-mail: liucr@tsinghua.edu.cn

Pickup probability of sediment incipience, which can account for the random nature of the sediment entrainment, is a desirable quantity to evaluate the sediment incipient motion under complex flows. Einstein (1942) defined the pickup probability for a bed particle as that of the instantaneous lift force larger than the effective weight force of the particle. And later on, the formulae to calculate the pickup probability were proposed by some researchers (Engelund and Fredsoe, 1976; Cheng, 1998). These formulae are related to the pickup probability with bed shear stress, while the effects of fluctuating pressure and the seepage are not considered. The works above did not mention the method to measure the pickup probability and the measured results. Recently, Dancey *et al*. (2002) presented an approach to measure the probability of bed particle moving quantitatively. In the study of Dancey *et al*. (2002), the concepts of observation period and the average period between the two adjacent turbulent events are introduced. However, the average period between the two adjacent turbulent events in the complex flow is difficult to be obtained.

In the present study, flows over a backward-facing step, in which separation and reattachment associated with large vortices can be found, are employed to study the probability of sediment particles movement under complex flows. A mathematical model considering the effects of fluctuating pressure and the seepage on the sediment incipient motion is presented to calculate the probability of sediment particle movement. A series of experiments are conducted to measure the instantaneous flow velocity fields and the probability of sediment particle movement downstream of the backward-facing step. The probability of sediment particle movement obtained by the theory is compared with the measured results. The roles of instantaneous bed shear stress and seepage flows induced by the bed pressure gradient on the sediment incipient are investigated. The possible scale of the turbulent events period is also discussed.

2. Mathematical Formulation

The sketch of the studied problem is shown in Fig. 1, x and y are the horizontal and vertical coordinates, z is pointing upward with its origin located at the sediment bed. The step is located at $x=0$, the height of the step is H_s, the vertical distance from the sediment bed to the bottom of the porous medium is H, and the water depth downstream of the step is D.

For the complex flows, the interaction of the large scale vortex with the bed can induce not only the shear stress but also a high pressure gradient on the bed, resulting in the seepage flow in the bed. The existence of the seepage enhances the sediment movement. Cheng and Chiew (1999) investigated the effect of upward bed seepage on the critical condition of sediment incipient motion, and gave the the critical shear velocities for uniform cohesionless sediment particles in the presence of upward seepage

$$\left[\frac{u_{*c}(i_{z0})}{u_{*oc}}\right]^2 = 1 - \frac{i_{z0}}{i_c}, \tag{1}$$

where u_{*oc} is the critical shear velocity without seepage, and i_c is the critical hydraulic gradient.

The incipient condition is:

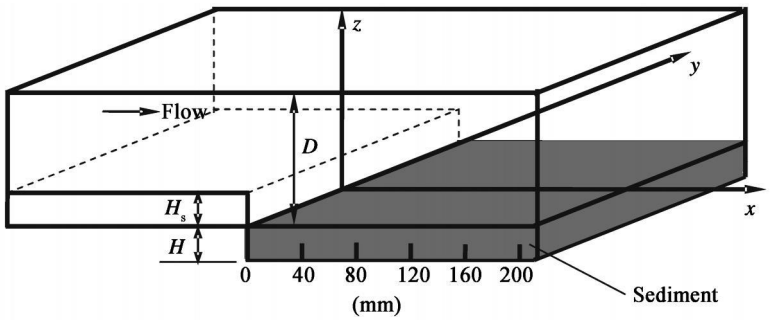

Fig. 1. Definition sketch.

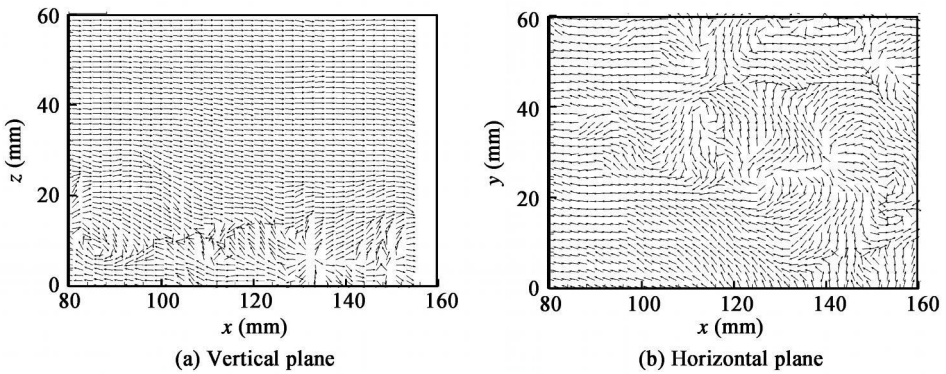

Fig. 2. Instantaneous flow velocity fields downstream of the step.

$$u_* > u_{*c}(i_{z0}) \tag{2}$$

where u_* and $u_{*c}(i_{z0})$ are the shear velocity of flow on the bed and critical shear velocity with seepage, respectively; i_{z0} is the vertical hydraulic gradient on the bed. For a horizontal bed, the value of u_{*oc} can be obtained by Shields diagram, and i_c is given by

$$i_c = \frac{\rho_s - \rho}{\rho}(1-\varepsilon), \tag{3}$$

where ρ_s and ρ are density of sediment particle and water respectively, and ε is the porosity of the sediment, see Cheng and Chiew (1999) for details.

According to critical incipient condition Eq. (2), the probability of sediment incipience can be expressed as:

$$P_i = \int_0^{\infty} P(u_* > u_{*c}(i_{z0}))f_{iz}(i_{z0})\,\mathrm{d}i_{z0}, \tag{4}$$

where $P(u_* > u_{*c}(i_{z0}))$ is defined as the probability of $u_* > u_{*c}(i_{z0})$, and $f_{iz}(i_{z0})$ is the probability density function of i_{z0}.

For the porous medium consisting of fine particles, the hydraulic gradient $i = \nabla h$ obeys Darcy's law:

$$v_s = Ki, \tag{5}$$

where v_s is the seepage velocity. Substituting Eq. (5) into the continuity equation $\nabla \cdot v_s = 0$ gives

$$\nabla^2 h = 0. \tag{6}$$

The hydraulic head h in the porous medium can be obtained by solving Eq. (6) with the following boundary conditions:

$$\begin{cases} h = h_0, z = 0 \\ \nabla h = 0, z = -H \end{cases} \tag{7}$$

where h_0 is the hydraulic head on the bed. As the quantities are classified into the mean and fluctuating components, the fluctuating hydraulic head $\tilde{h}$ must satisfy the following governing equation and boundary conditions:

$$\begin{cases} \nabla^2 \tilde{h} = 0 \\ \tilde{h} = \tilde{h}_0, z = 0 \\ \nabla \tilde{h} = 0, z = -H \end{cases} \tag{8}$$

where the tilde represents the fluctuating component. The solutions of Eq. (8) can be given as:

$$\tilde{h} = \int_{-\infty}^{\infty}\int_{-\infty}^{\infty} \frac{\cosh[(\sqrt{k_x^2 + k_y^2})(H + z)]}{\cosh[(\sqrt{k_x^2 + k_y^2})H]} F(k_x, k_y, t) e^{i2\pi(k_x x + k_y y)} dk_x dk_y, \tag{9}$$

$$F(k_x, k_y, t) = \int_{-\infty}^{\infty}\int_{-\infty}^{\infty} \tilde{h}_0(x, y, t) e^{-i2\pi(k_x x + k_y y)} dx dy. \tag{10}$$

The fluctuating vertical hydraulic gradient in the region near the bed can be obtained with Eq. (9):

$$\tilde{i}_{z0} = \int_{-\infty}^{\infty}\int_{-\infty}^{\infty} (\sqrt{k_x^2 + k_y^2}) F(k_x, k_y, t) e^{i2\pi(k_x x + k_y y)} dk_x dk_y. \tag{11}$$

The variance of the random variable i_{z0} can be expressed as:

$$\sigma_{i_z}^2 = E\left[\int_{-\infty}^{\infty}\int_{-\infty}^{\infty}\int_{-\infty}^{\infty}\int_{-\infty}^{\infty} (k_x^2 + k_y^2) \left| F(k_x, k_y, t) \right|^2 e^{i2\pi(k_x x + k_y y)} e^{-i2\pi(k_x' x + k_y' y)} dk_x dk_y dk_x' dk_y'\right] \tag{12}$$

where $E[X]$ denotes the mean of X. From Eq. (11), the fluctuating horizontal hydraulic gradient on the bed can be given as:

$$\tilde{i}_{x0} = \int_{-\infty}^{\infty}\int_{-\infty}^{\infty} k_x F(k_x, k_y, t) e^{i2\pi(k_x x + k_y y)} dk_x dk_y; \tag{13}$$

$$\tilde{i}_{y0} = \int_{-\infty}^{\infty}\int_{-\infty}^{\infty} k_y F(k_x, k_y, t) e^{i2\pi(k_x x + k_y y)} dk_x dk_y. \tag{14}$$

Substituting Eqs. (13) and (14) into Eq. (12), one can obtain

$$\sigma_{i_z}^2 = \sigma_{i_x}^2 + \sigma_{i_y}^2 \tag{15}$$

$$\sigma_{i_x}^2 = E\left[\int_{-\infty}^{\infty}\int_{-\infty}^{\infty}\int_{-\infty}^{\infty}\int_{-\infty}^{\infty} k_x^2 \left| F(k_x, k_y, t) \right|^2 e^{i2\pi(k_x x + k_y y)} e^{-i2\pi(k_x' x + k_y' y)} dk_x dk_y dk_x' dk_y'\right] \tag{16}$$

$$\sigma_{i_y}^2 = E\left[\int_{-\infty}^{\infty}\int_{-\infty}^{\infty}\int_{-\infty}^{\infty}\int_{-\infty}^{\infty} k_y^2 \left| F(k_x, k_y, t) \right|^2 e^{i2\pi(k_x x + k_y y)} e^{-i2\pi(k_x' x + k_y' y)} dk_x dk_y dk_x' dk_y'\right] \tag{17}$$

where $\sigma_{i_x}^2$ and $\sigma_{i_y}^2$ are the variances of the random variables i_{x0} and i_{y0}, respectively.

Assuming that the probability distribution of i_{z0} obeys normal distribution

$$f_{i_z}(i_{z0}) = \frac{1}{\sigma_{i_z}\sqrt{2\pi}} e^{-i_{z0}^2/\sigma_{i_z}^2}. \tag{18}$$

The probability of sediment incipience can be obtained with Eq. (4) as $\sigma_{i_x}^2$, $\sigma_{i_y}^2$ and u_* are known. The values of $\sigma_{i_x}^2$, $\sigma_{i_y}^2$ and u_* can be derived from the instantaneous flow velocity fields above the bed, which will be discussed in the following section.

3. Analysis of Experimental Data

The flow field experiments were carried out in a perspex flume, which had a test section of 6 m long, 0.4 m wide and 0.4 m deep. In our experiments, the working water depth was fixed at 0.3 m. Turbulent intensity at the inlet of the flume was lower than 0.3% and the adjustable flow velocity could vary continually from 0.05 m/s to 1.0 m/s. A step with the height of 2.5 cm was placed in the central region of the flume. The instantaneous velocity fields were measured by the PIV (particle image velocimetry). The resolution of the CCD camera used in the PIV system was 640×480 pixels and the grabbing speed was 200 frames per second. Separate sets of experiments were also carried out to study the probability of sediment incipience. To prepare the sediment bed, a sediment container was arranged downstream of the step and uniform glass beads with density 2500 kg/m^3 and diameter 0.165 mm were filled in the sediment container. The porosity of the sediment bed was about 0.41. For the measurement of the number of moving particles in the observation period, a CCD camera of resolution 768×576 pixels was placed above the flow to record images of sediment particles through a horizontal, transparent plate whose lower surface was adjusted to touch the water surface. The CCD camera used in the sediment incipient experiment can grab up to 25 frames per second. Details of the experiments were given in Liu *et al*. (2008). The instantaneous velocity fields measured in the horizontal plane near the bed are used to calculate the instantaneous bed shear velocity and horizontal hydraulic gradient on the bed. The number of moving particles in the observation period is used to analyze the sediment incipient probability.

3.1 Bed Shear Velocity

As the instantaneous flow velocity in the horizontal plane above the bed are given, the bed shear velocity u_* can be obtained by solving the following equations (Zhou *et al*., 1993)

$$\begin{cases} \dfrac{u_b}{u_*} = \dfrac{u_* z_b}{\nu}, & \dfrac{u_* z_b}{\nu} < 5 \\ \dfrac{u_b}{u_*} = 5.0\ln\dfrac{u_* z_b}{\nu} - 3.05, & 5 < \dfrac{u_* z_b}{\nu} < 30 \\ \dfrac{u_b}{u_*} = 2.5\ln\dfrac{u_* z_b}{\nu} + 5.5, & \dfrac{u_* z_b}{\nu} > 30 \end{cases} \tag{19}$$

where z_b is the vertical distance of the measured plane away from the bed and u_b is the flow velocity magnitude in the measured plane. Eq. (19) is valid only if $u_* z_b/\nu$ is smaller than a certain value,

which depends on flow cases. For the backward-facing step flow, where the intensity of the vortex is high, a small z_b must be chosen. In the experiment of Liu *et al.* (2008), z_b= 0.5 mm, which ensures $u_* z_b/\nu < 30$.

3.2 Bed Horizontal Hydraulic Gradient

The pressure gradient can be obtained by solving the Navier-Stokes equation:

$$\nabla p = -\rho\left(\frac{\partial \vec{u}}{\partial t} + \vec{u}\cdot\nabla\vec{u} + g\vec{k}\right) + \mu\nabla^2\vec{u}, \tag{20}$$

where $\vec{u}$ is the instantaneous flow velocity. Landau and Lifshitz (1987) conclude that, for the large eddies which are the basis of any turbulent flow, the viscosity is unimportant. As the pressure gradient is calculated in the high Reynolds number turbulent flow, the viscosity can be ignored:

$$\nabla p = -\rho\left(\frac{\partial \vec{u}}{\partial t} + \vec{u}\cdot\nabla\vec{u} + g\vec{k}\right). \tag{21}$$

The horizontal hydraulic gradient on the bed can be approximately calculated by the horizontal pressure gradient near the bed:

$$\begin{cases} i_{x0} = \dfrac{1}{\rho g}\dfrac{\partial p(x, y, z_b, t)}{\partial x} \\ i_{y0} = \dfrac{1}{\rho g}\dfrac{\partial p(x, y, z_b, t)}{\partial y} \end{cases} \tag{22}$$

As a result of flattening of eddies near the bed, the horizontal velocity is amplified and the vertical velocity is sharply attenuated. The horizontal velocity can be much larger than the vertical velocity when the distance apart from the bed is much smaller than the length scale of eddies (Hannoun, 1988). Ignoring the vertical flow velocity near the bed and substituting Eq. (22) into Eq. (21), the following formulae can be obtained:

$$\begin{cases} i_{x0} = -\dfrac{1}{g}\left(\dfrac{\partial u}{\partial t} + u\dfrac{\partial u}{\partial x} + v\dfrac{\partial u}{\partial y}\right) \\ i_{y0} = -\dfrac{1}{g}\left(\dfrac{\partial v}{\partial t} + u\dfrac{\partial v}{\partial x} + v\dfrac{\partial v}{\partial y}\right) \end{cases} \tag{23}$$

where u and v are x- and y-components of the flow velocity at the horizontal plane $z = z_b$.

3.3 Definition of the Incipient Probability

According to the argument of Dancey (2002), the sediment incipient motion is due to the turbulent events. Denoting the fraction of sediment moving in the observation period T_o as Γ_m, Dancey (2002) gives the sediment incipient probability P_i

$$P_i = \frac{\Gamma_m T_t}{T_o}, \tag{24}$$

where T_t is the average period between the two adjacent turbulent events. It must be noted that the expression (24) is suitable for the case of large T_o ($T_o > T_t$). For small T_o ($T_o < T_t$), we have $P_i = \Gamma_m$. Unfortunately, the appropriate scaling of the turbulent events period is unsolved up to now. In the present study, the fraction of sediment moving in the observation period T_o= 0.04 s (due to the limi-

tation of the hardware) obtained by Liu *et al*. (2008) is presented and compared with the sediment incipient probability obtained with Eq. (4). The possible scale of the turbulent events period is discussed.

4. Results and Discussion

4.1 Flow Fields

The velocity fields for backward-facing step with three different Reynolds numbers Re ($Re = U_0 H_s/\nu$, U_0 being the mean velocity at inlet of the fluid) have been studied by PIV. The instantaneous velocity field at $Re = 5000$ ($U_0 = 0.2$ m/s) is reported here. Over a time interval of 3 s, 600 image frames are grabbed so that the instantaneous velocity fields at 600 times can be obtained. Fig. 2 shows the instantaneous velocity fields in the vertical and horizontal plane. The complex vortex structures can be observed in both vertical and horizontal plane, which implies three dimensional vortex structures exist downstream of the step.

For the verification of the validation of the PIV measurements, the measured velocity and the root mean square velocity are compared with the DNS (direct numerical simulation) results of Le *et al*. (1997). Fig. 3 shows the mean streamwise velocity profiles on the vertical plane at three different locations downstream of the step. A good agreement of our PIV measurements with the DNS results of Le *et al*. (1997) can be obtained. The statistic average reattachment length in our experiments is found to be about $6H_s$, which agrees with the results of Armaly *et al*. (1983) and Le *et al*. (1997).

The root mean square velocity profiles of longitudinal and vertical velocity fluctuations ($(\overline{u'^2})^{1/2}$, $(\overline{w'^2})^{1/2}$) at three different locations downstream of the step ($x/H_s = 4, 6, 10$) are shown in Fig. 4 and Fig. 5, respectively. A comparison of the root mean square velocity obtained by our PIV with that of Le *et al*. (1997) at locations of $x/H_s = 4$ and 6 shows that our PIV results agree well with the DNS results of Le *et al*. (1997) in the region near the bed ($z < 0.3H_s$). However, a large discrepancy between our PIV results and the DNS results occurs in the region far from the bed ($z > 0.3H_s$), which can be explained by the long time interval of two image frames used in PIV measurements. The time interval of two image frames that is suitable for the measurement in the region near the bed may lead to large errors of that in the region far from the bed, as the fluid velocity far from the bed is higher than that near the bed. Fortunately, the sediment incipient motions are mainly related to the flow characteristics near the bed, which ensure that our PIV measurements can be used to analyze the sediment incipient probability. According to our PIV measurements, it is found that the longitudinal velocity fluctuation intensity is higher than the vertical one and the maximum root mean square velocity near the bed occurs in the region near the reattachment point.

The instantaneous velocity fields in the horizontal plane 0.5 mm away from the bed for 600 times are used to calculate the instantaneous bed shear velocity by Eq. (19). Analyzing 600 velocity fields in the region $x_0 - 5$ mm $< x < x_0 + 5$ mm, we obtain about 84000 values of u_*. By counting the number of $u^* > u_0$ in these 84000 values, the probability that the bed shear velocity is larger than

u_0, $P(u_* > u_0)$ at $x = x_0$ can be obtained. Fig. 6 shows the value of $P(u^* > u_0)$ at the locations $x/H_s = 2, 6, 8, 12$, respectively. The instantaneous bed shear velocity has a large value far downstream of the step ($x/H_s = 12$) and the probability of a low bed shear velocity occurrence is not large in this region. In the region near the reattachment point ($x/H_s = 6, 8$), the probability of a low bed shear velocity occurrence becomes large, however, a high bed shear velocity can also be found. In the region near the step ($x/H_s = 2$), the bed shear stress becomes very low and the probability of a high bed shear velocity occurrence is very small. The probability distribution of the bed shear velocity obtained by this study can be explained by the characteristics of the backward-facing step flow. The large probability of the high bed shear velocity occurrence far downstream of the step may be attributed to the high mean flow velocity near the bed. Near the attachment point, the mean flow velocity near the bed approaches zero, while the velocity fluctuation intensity reaches its maximum value, both high and low bed shear velocities can occur. The low mean flow velocity near the bed and also the low velocity fluctuation intensity in the region near the step may account for the low bed shear velocity in this region.

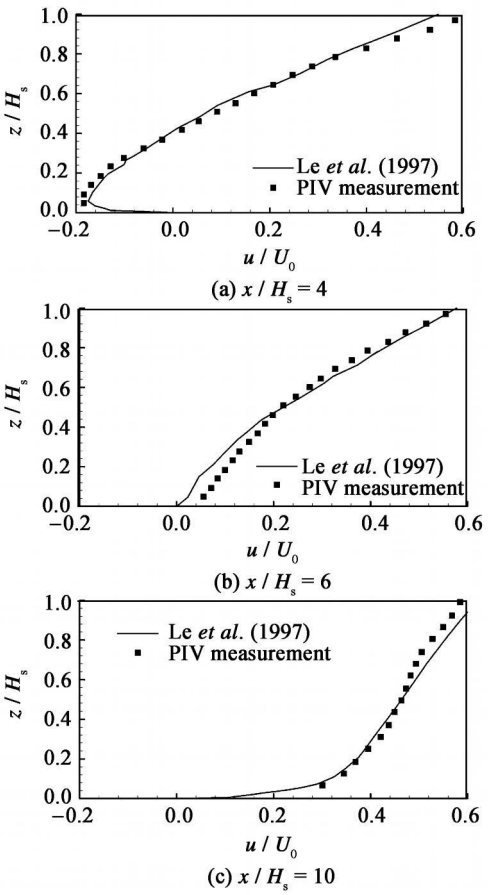

Fig. 3. Mean streamwise velocity profiles on the vertical plane.

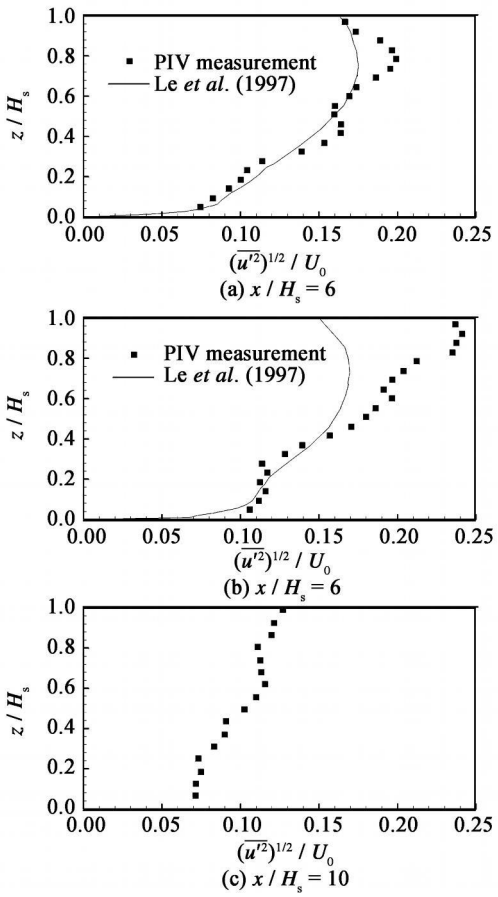

Fig. 4. Root mean square velocity profiles of longitudinal velocity fluctuations.

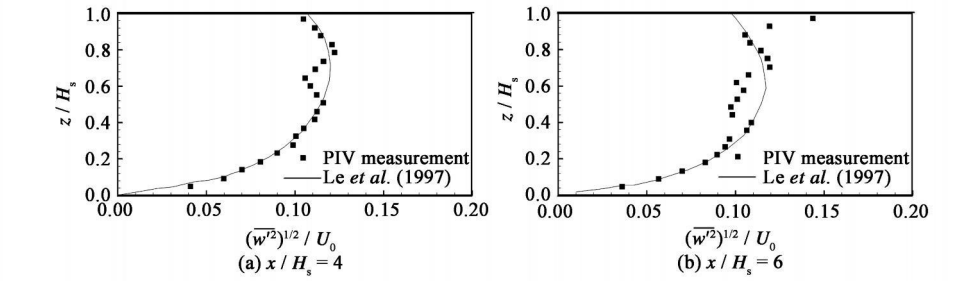

Fig. 5. Root mean square velocity profiles of vertical velocity fluctuations.

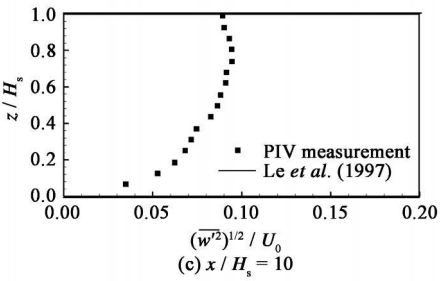

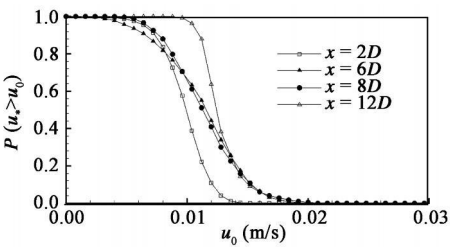

Fig. 6. Probability of the bed shear velocity being larger than u_0.

The instantaneous velocity fields in the horizontal plane 0.5 mm away from the bed at 600 times were also used to calculate the instantaneous horizontal hydraulic gradients on the bed by Eq. (23). The velocity fields at two times with interval of 0.005 s were used to calculate $\frac{\partial u}{\partial t}$ and $\frac{\partial v}{\partial t}$, and the velocity fields with 38 × 28 velocity vectors in the region of 80 mm × 60 mm at one time were used to calculate $u\frac{\partial u}{\partial x}$, $u\frac{\partial v}{\partial x}$, $v\frac{\partial u}{\partial y}$, and $v\frac{\partial v}{\partial y}$. Then the instantaneous horizontal hydraulic gradients i_{x0} and i_{y0} on the bed were obtained. Analyzing 600 velocity fields in the region $x_0 - 5$ mm$< x < x_0 + 5$ mm, we can obtain about 84000 values of i_{x0} and i_{y0}. By counting the number of $i_x - 0.02 < i_{x0} < i_x + 0.02$ (or $i_y - 0.02 < i_{y0} < i_y + 0.02$) in region $x_0 - 5$ mm$< x < x_0 + 5$ mm, the probability density function (PDF) of the random variable i_{x0} (or i_{y0}) at the position $x = x_0$ can be given approximately. Fig. 7 shows the PDF of the horizontal hydraulic gradients on the bed at the positions $x/H_s = 2$, 6, 8, 12, respectively. It is found that the experiment probability distribution of i_{x0} and i_{y0} obeys normal distribution, which verify the validation of the assumption about the probability distribution of i_{x0} given in Eq. (18). According to the PDF of the horizontal hydraulic gradients, the values of $\sigma_{i_x}^2$ and $\sigma_{i_y}^2$ are given (as shown in Fig. 7). The maximum values of $\sigma_{i_x}^2$ and $\sigma_{i_y}^2$ occur at a location $6H_s$ away from the step, which is the location of the reattachment point. Recalling the discussion above, the maximum

velocity fluctuations near the bed also appear in the region near the reattachment point, which implies larger velocity fluctuations may induce larger fluctuations of hydraulic gradients.

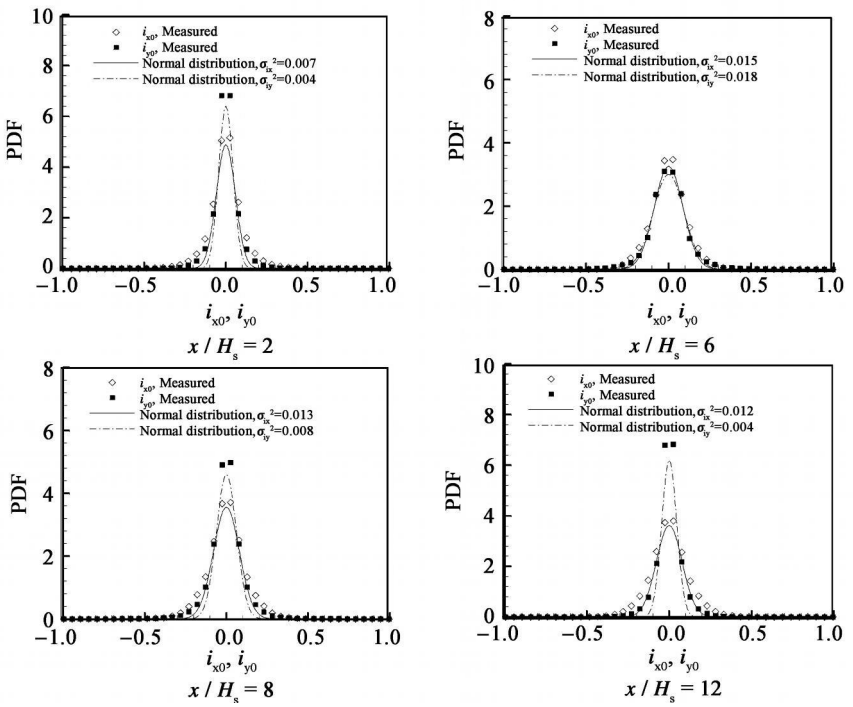

Fig. 7. Probability density function of the horizontal hydraulic gradients on the bed.

4.2 Sediment Incipient Probability

The initial shear velocity formula presented by Dou (2000) gives the critical shear velocity without seepage u_{*oc}= 0.016 m/s (for little motion) and Eq. (3) gives the critical hydraulic gradient i_c = 0.885. Fig. 8 gives the sediment incipient probability obtained from Eq. (4) and the fraction of sediment moving in the observation period T_o= 0.04 s given by Liu *et al*. (2008). In order to study the effects of seepage on the sediment incipience, the sediment incipient probability in the case that the effects of seepage are not considered is also presented in Fig. 8.

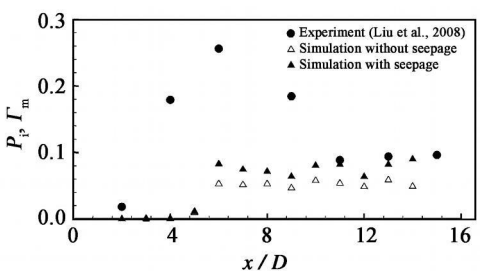

Fig. 8. Sediment incipient probability and the fraction of sediment moving in the observation period.

It can be seen that the sediment incipient probability in the case that the effects of seepage are considered is about 50% higher than that in the case that the effects of seepage are not considered.

Comparing the sediment incipient probability obtained with Eq. (4) and the fraction of sediment moving in the observation period obtained by Liu *et al.* (2008), we can observe that they are in a good agreement downstream of the reattachment point ($x/H_s > 10$) and have a discrepancy in the region near the reattachment point ($4 < x/H_s < 10$), which may be explained by analyzing the flow structure downstream of the step.

For backward-facing step flow, the free-shear layer shedding from the step forms vortices due to Kelvin-Helmholtz (KH) instability. As the free-shear layer rolls up, the vortices continue to grow and interact with the bed near the reattachment point. Thus, the turbulence has fully developed in the region near the reattachment point so that high intensity small-scale vortices will form in this region. Owing to the existence of the high intensity small-scale vortices, the period between the two adjacent turbulent events may be very short. Furthermore, the high intensity small-scale vortices can induce the vertical flow velocity near the bed, which is ignored in the calculation of the horizontal hydraulic gradient on the bed. So the existence of high intensity small-scale vortices can explain why the fraction of sediment moving in the observation period may be much higher than the sediment incipient probability predicted near the reattachment point in theory.

The energy of the small-scale vortices generated in the free-shear layer is dissipated downstream of the reattachment point, which may result in a long period between the two adjacent turbulent events. The inner scale of the bursting period T_B, which is obtained by Shah and Antonia (1989) in turbulent boundary layer flow, is used to estimate the period between the two adjacent turbulent events for the flow downstream of reattachment point in this study. Shah and Antonia (1989) gave a normalized bursting period $T_B^+ = T_B u_*^2 / \nu$, which ranges from 50 to 250. In the present study, the bed shear velocity u_* downstream of the reattachment point ranges from 0.01 to 0.02 m/s. It can be estimated that the average period between the two adjacent turbulent events is about 0.125 ~ 2.5 s, which is larger than the observation period T_o. Thus, the fraction of sediment movement in the observation period downstream of the reattachment point equals the sediment probability. It is not surprising that sediment incipient probability obtained with Eq. (4) agrees well with the fraction of sediment moving in the observation period downstream of the reattachment point.

5. Conclusions

The instantaneous bed shear velocity and the pressure gradient on the bed are given and the effects of the fluctuating pressure and the seepage on the sediment incipient probability are studied in this paper. The following conclusions can be drawn.

(1) The instantaneous pressure gradient on the bed obeys normal distribution.

(2) The sediment incipient probability in consideration of the effects of seepage is about 50% higher than that without consideration of the effects of seepage. The sediment incipient probability in consideration of the effects of seepage agrees well with the measured results downstream of the reattachment point.

(3) In the region near the reattachment point, the sediment incipient probability obtained by the

oretical model is lower than the measured results. The reason may be the existence of high intensity small-scale vortices in the region near the reattachment point. In order to understand the incipient motion of sediment in the region near the reattachment point, the behavior of the small-scale vortices must be studied further.

References

Armaly, B. F., Durst, F., Pereira, J. C. F. and Schonung, B., 1983. Experimental and theoretical investigation of backward-facing step, *J. Fluid Mech.*, **127**, 473~396.

Cao, Z., Pender, G. and Meng, J., 2006. Explicit formula of the Shields diagram for incipient motion of sediment, *Journal of Hydraulic Engineering*, ASCE, **132**(10): 1097~1099.

Chen, G. P., Zuo, Q. H. and Huang, H. L., 2004. Local scour around piles under wave action, *China Ocean Eng.*, **18**(3): 403~412.

Cheng, N. S. and Chiew, Y. M., 1998. Pickup probability for sediment entrainment, *Journal of Hydraulic Engineering*, ASCE, **124**(2): 232~235.

Cheng, N. S. and Chiew, Y. M., 1999. Incipient sediment motion with upward seepage, *Journal of Hydraulic Research*, **37**(5): 665~681.

Cheng, N. S., 2004. Analysis of bed load transport in laminar flow, *Advance in Water Resources*, **27**(9): 937~942.

Dancey, C. L., Diplas, P., Papanicolaou, A. and Bala, M., 2002. Probability of individual grain movement and threshold condition, *Journal of Hydraulic Engineering*, ASCE, **128**(12): 1069~1075.

Dou, G. R., 2000. Incipient motion of sediment under currents, *China Ocean Eng.*, **14**(4): 391~406.

Einstein, H. A., 1942. Formula for the transportation of bed load, *Trans.* ASCE, **107**, 561~597.

Engelund, F. and Fredsoe, J., 1976. A sediment transport model for straight alluvial channels, *Nordic Hydro.*, **7**, 293~306.

Hannoun, I. A., Fernando, H. J. S. and List, E. J., 1988. Turbulence structure near a sharp density interface, *J. Fluid Mech.*, **189**, 189~209.

Landau, L. D. and Lifshitz, E. M., 1987. *Fluid Mechanics*, Pergamon Press.

Le, H., Moin, P. and Kim, J., 1997. Direct numerical simulation of turbulent flow over a backward-facing step, *J. Fluid Mech.*, **330**, 349~374.

Liang, D. F., Cheng, L. and Li, F. J., 2005. Numerical modeling of flow and scour below a pipeline in currents, Part II. Scour simulation, *Coast. Eng.*, **52**(1): 43~62.

Liu, C. R. and Huhe, A. D., 2003. Homogenous turbulence structure near the wall and sediment incipience, *The Ocean Engineering*, **21**(3): 50~55. (in Chinese)

Liu, C. R., Deng, L. Y., Huang, Z. H. and Huhe, A. D., 2008. Experimental study of sediment incipience under complex flows, *Trans. Tianjin Univ.*, **14**(4): 300~306.

Lyn, D. A., 1995. Observation of initial sediment motion in a turbulent flow generated in a square tank by a vertically oscillating, *Water Resource Engineering, Proceedings of the First International Conference*, Vol. 1, San Antonio, Texas, ASCE, 609~613.

Rijn, L. C. V., 1984, Sediment transport, part III: Bed forms and alluvial roughness, *Journal of Hydraulic Engineering*, ASCE, **110**(12): 1733~1754.

Shah, D. A. and Antonia, R. A., 1989. Scaling of the bursting period in turbulent boundary layer and duct flows, *Physics of Fluids A*, **1**(2): 318~325.

Zhao, M. and Teng, B., 2001. Numerical simulation of local scour around a large circular cylinder under wave action, *China Ocean Eng.*, **15**(3): 371~382.

Zhou, G. T., Yan, Z. Y., Xu, S. X. and Zhang, K. B., 1993. *Fluid Mechanics*, Higher Education Press. (in Chinese)

Zhou, Y. R., Chen, Y. P. and Ma, Q. N., 2001. Threshold of sediment movement in different wave boundary layers, *China Ocean Eng.*, **15**(4): 509~520.